Temperature insensitive delay-line fiber interferometer operating at room temperature

Bo Shi, Guiseppe Marra, Zitong Feng, Hesham Sakr, John R. Hayes, Eric R. Numkam Fokoua, Meng Ding, Francesco Poletti, David J. Richardson, and Radan Slavík

***Abstract*—Environmental temperature fluctuations cause phase changes of the light propagating through optical fibers due to their thermal sensitivity. This limits the stability of fiber delay-line interferometers. Here, we present a thermally-insensitive fiber Mach-Zehnder interferometer. It consists of a hollow core fiber (HCF), which has a low thermal sensitivity coefficient, in one branch and a standard single-mode fiber with a thermal sensitivity coefficient about 25 times larger in the other. By setting their associated length ratio to approximately 25:1, the optical phase of the light in both arms changes by the same amount with temperature, making the difference in their optical paths insensitive to temperature and thus producing thermally-insensitive interference. As the thermal sensitivity coefficient of the optical fibers is itself slightly temperature dependent, exactly-zero sensitivity is achieved at a specific temperature only. We show how this zero-sensitivity temperature can be controlled via control of the relative fiber lengths in the two interferometer arms and set it to room temperature. Further, we show that our interferometer is over 100 times less sensitive to temperature than a single-mode fiber-based interferometer over temperature range as large as 25-50°C. When considering a simple temperature control that keeps the interferometer within ±1°C, the demonstrated interferometer achieves over 2000 times lower thermal sensitivity than a single-mode fiber-based interferometer and over 100 times lower sensitivity than an HCF-only based interferometer. Finally, we discuss how the thermal sensitivity of such interferometer depends on the light source wavelength.**

***Index Terms*—Optical fiber interferometer, hollow core fiber, optical fibers, thermal sensitivity**

I. Introduction

Optical delay-line interferometers produce interference between a signal and a delayed copy. They find applications in many areas such as ultra-stable laser locking [1][2], optical filtering [3], and precision optical sensing including gravitational wave detection [4] and tests of relativity [5].

When built with optical fibers, delay-line interferometers are lightweight, alignment-free, and can provide a very long delay (e.g., kilometers of fiber). However, interferometers made of standard single-mode optical fibers (SSMF) suffer from relatively high sensitivity to environmental temperature variations. This is mainly due to the thermo-optic coefficient of the fiber silica glass core, which makes the effective refractive index n_{eff} of the fiber mode relatively sensitive to temperature. The accumulated phase $\varphi = 2\pi n_{eff} L/\lambda$ (L: fiber length; λ: light wavelength in vacuum) in the individual interferometer arms then changes with temperature, causing the interferometer interference fringes to drift over time [6].

The fiber thermal sensitivity coefficient S_φ defined as the temperature sensitivity of the accumulated phase φ normalized to the fiber length L is given by:

$$S_\varphi = \frac{1}{L}\frac{d\varphi}{dT} = \frac{2\pi}{L\lambda}\frac{d(n_{eff}L)}{dT} = \frac{2\pi}{\lambda}\left(\frac{dn_{eff}}{dT} + \frac{n_{eff}}{L}\frac{dL}{dT}\right), \tag{1}$$

where T is temperature. The first term on the Eq. (1) right-hand side is due to the glass core thermo-optic effect and accounts for about 95% of the thermal sensitivity coefficient in SSMF [7]. The second term describes the effect of fiber thermal expansion. SSMF's S_φ has been reported to be as high as 48 rad/m/K at a wavelength of 1550 nm [8]. Considering a delay-line interferometer with 100 m fiber delay subject to 1-mK temperature change (which is already challenging to be achieved in practice), the phase would drift by as much as 4.8 radians, which corresponds to almost one full interference fringe drift. To achieve stable interference, sub-mK temperature stabilization would be needed. Provided such interferometer is used for laser locking to reduce its phase noise [1], temperature variation as small as 20 mK would produce significant frequency instability of 3×10^{-12} at 1- averaging [1]. To decrease the negative impact of the fiber's thermal sensitivity, temperature needs to be controlled at unpractical levels

Manuscript recoeved ** **, 2022; revised ** **, 2022; Accepted ** **, 2022. Date of publication ** **, 2022; data of current version ** *, 2022. This work was supported by EPSRC project "Airguide Photonics,' under grant EP/P030181/1. The work of Bo Shi was supports by CSC scholarship. The work of Radan Slavík was supports by RAEng Fellowship. *(Corresponding author: Bo Shi)*

Bo Shi, Zitong Feng, Hesham Sakr, John R. Hayes, Eric R. Numkam Fokoua, Meng Ding, Francesco Poletti, David J. Richardson, and Radan Slavík are with the Optoelectronic Research Centre, University of Southampton, SO17 1BJ Southampton, U.K. (e-mail: s.bo@soton.ac.uk; Zitong.Feng@soton.ac.uk; H.Sakr@soton.ac.uk; jrh@orc.soton.ac.uk ; eric.numkam-fokoua@soton.ac.uk; M.Ding@soton.ac.uk ; frap@orc.soton.ac.uk; djr@orc.soton.ac.uk; r.slavik@soton.ac.uk)

GuiseppeMarra is with the National Physical Laboratory, Hampton Rd., Teddington, TW11 0LW, U K (e-mail: giuseppe.marra@npl.co.uk)

Mentions of supplemental materials and animal/human rights statements can be included here.

Color versions of one or more of the figures in this article are available online at http://ieeexplore.ieee.org

(e.g., sub-mK). Alternatively, the thermal sensitivity of optical fibers can be reduced.

It can be reduced by using fibers with a specialty coating that contracts with a temperature increase [9], using core material that has a reduced thermo-optic coefficient [10] or using hollow core fibers (HCFs) [7]. In HCF, light is guided through the central hole rather than silica glass, eliminating 95% of the fiber's S_φ [7]. Specialty coated fibers were reported to have S_φ as low as 4.4 rad/K/m [9], specialty-doped core fibers 38 rad/m/K [11], and HCFs 2.4 rad/m/K [8], all achieved at room temperature. Several approaches have been proposed to further reduce or even eliminate this sensitivity. In SSMF, cooling to -250°C was shown to lead to $S_\varphi = 0$ [12]. In HCF, this was also demonstrated, but at a significantly easier-to-reach temperature of -71°C [13], where silica glass coefficient of thermal expansion crosses zero. Another approach is using open-ended HCF [14] in which fiber elongation is compensated by the reduced refractive index of the fiber core due to temperature-induced pressure change and associated molecules escaping or entering the HCF core. At atmospheric pressure, it led to a zero thermal sensitivity coefficient at a temperature of 107°C. As far as achieving this at room temperature is concerned, reduction in the fibers thermal sensitivity coefficient was suggested, e.g., by winding HCF around a thermally-insensitive bobbin under tension, where temperature variations caused a change in fiber tension, but not length [15]. Although in principle this approach could achieve $S_\varphi = 0$, so far it has been demonstrated to reduce it only by a factor of three. Additionally, use of a thermally-insensitive bobbin increases weight, which may be undesirable in interferometers for some applications e.g., for use in aerospace.

Besides direct reduction of the fiber's S_φ as discussed above, the stability of a delay-line interferometer can also be improved by making the two arms from materials with different S_φ and their lengths chosen to induce the same phase change in both arms when subject to a temperature change, Fig. 1. This has been already demonstrated in integrated optic Mach-Zehnder interferometers [16] and also in our preliminary study [17] in which we used a HCF in one arm and an SSMF in the other. The S_φ of HCF is significantly (~30 times) lower than that of SSMF, so the same thermal sensitivity should be achieved in both arms when the HCF is approximately 30 times longer than the SSMF. Inserting such a relatively short length of SSMF into the reference arm of an HCF delay-line interferometer makes the reduction of the delay between the two interferometer arms negligible. We refer to this arrangement as a "compensated delay-line interferometer".

Here we present a compensated delay-line interferometer, building on our preliminary work [17]. Besides giving more details including the importance of the fiber coating, we show how the zero-sensitivity operating temperature can be tuned and demonstrate setting it close to room temperature. Furthermore, we increase the delay imbalance in the interferometer to increase its phase sensitivity which is desirable in applications such as laser locking [1]. And we verify results obtained by using two different measuring methods. Additionally, we discuss how the thermal sensitivity of the interferometer changes with temperature, which influences the temperature range over which it has a very low thermal sensitivity, e.g., 2000 times smaller than an interferometer made solely of SSMF. Finally, we discuss how the interferometer thermal sensitivity changes with wavelength.

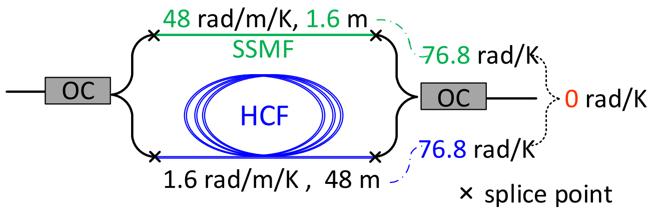

Fig. 1. Principle of the compensation method. Optical signals propagating in both interferometer arms experience the same phase shift when the ambient temperature changes. SSMF: standard single-mode fiber; HCF: hollow-core fiber; OC: optical coupler.

II. Experimental Setup

The experimental set-up we used to measure the thermal sensitivity is shown in Fig. 2. A narrow linewidth laser (RIO Orion from Luna Innovations, USA, emitting at 1558 nm) was frequency-locked to a carrier-envelope offset (CEO) stabilized optical frequency comb. This stabilization was required to suppress long-term laser frequency fluctuations that could produce interference fringe drift at the output of the interferometer and be confused with the thermally-induced phase change in the fibers. The HCF used in this experiment was manufactured in-house and is based on a Nested Antiresonant Nodeless Fiber (NANF) geometry [18] with a glass silica jacket tube of 185/70 µm outer/inner diameter. The SSMF was also manufactured in-house. In our initial experiments (not shown here), we found the performance of the compensated interferometer was limited by hysteresis in the optical path length variation due to the visco-elastic properties of the fiber coating [19]. Due to coating viscoelasticity, the phase of light propagating through a length of fiber keeps changing even after a stable temperature has been achieved, with a time constant of up to 60 000 s [19]. As this effect has different dynamics and magnitude in the HCF and SSMF (different coating thicknesses, non-identical coating on both fibers, different effect on the effective refractive indices for SSMF and HCF, etc.), the compensation of one arm with respect to the other depended on the rate of temperature change and took long time to settle. To avoid this, we fabricated the fibers with a very thin coating d (about 10 µm coating thickness). We have demonstrated earlier that this thickness significantly reduces the hysteresis in the HCF [20]. To distinguish a generic SSMF with our thinly coated SSMF, we refer to it as T-SSMF with 'T' for "thin coating". We adopt the same notion for our HCF (T-HCF).

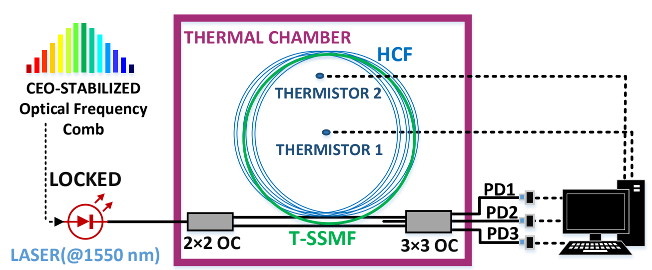

Fig. 2. Measurement set-up to characterize the thermal sensitivity of delay-line interferometers. OC: optical coupler; PD: photodetector; CEO: Carrier-Envelope Offset.

We coiled fibers freely (without any spool) in both short and long arms together with a diameter of 14 cm, and spliced them to a 2×2 input coupler and a 3×3 output coupler, both made of SSMF to form a Mach-Zehnder interferometer. The couplers' SSMF tails were cut to the same length of 1.2 m with an accuracy of 5 mm, and placed together. Thus, any phase change in the tails due to temperature should be identical in both interferometer arms and thus cancel out. The 3×3 output coupler enables un-ambiguous phase change extraction including its sign [21]. We put the interferometer into a thermal chamber and placed a thermistor in the center of the coiled fibers, Fig. 2. Three delay-line interferometers were built and tested in this chamber. The first two were not compensated interferometers and were used to measure the thermal sensitivity S_φ of our T-SSMF and T-HCF, respectively. They had 1.6-m T-SSMF and 40-m of T-HCF spliced in between the pigtails of the two couplers in the delay arm, respectively, while the coupler pigtails in the other arm were spliced directly together. As the pigtails in both interferometer arms were cut to the same length, the delay in these two interferometers was determined by the 1.6-m T-SSMF and 40-m of T-HCF only. We measured the thermal sensitivity S_φ of 1.57 rad/m/K for the T-HCF [20] and 39.3 rad/m/K for T-SSMF at 28°C. We give more details about these measurements later. For the available 40 m length of T-HCF, a 1.6-m long T-SSMF was thus required to produce the same phase change in response to temperature (length ratio of 1:25). The third interferometer was the compensated delay-line interferometer with the 40 m T-HCF in the delay arm and 1.6 m T-SSMF in the other arm.

We used two methods to measure the thermal sensitivity of delay-line interferometers. The first one was based on recording the accumulated phase with temperature as it continuously changed over a large range (e.g. 10-60°C). Subsequently, we fitted the measured accumulated phase and differentiated it to obtain the thermal sensitivity. We refer to this as the dynamic measurement. The second method was based on measuring the accumulated phase between two temperatures which have a small difference (e.g. 30-32°C), calculating the accumulated phase difference and dividing it by the temperature change. We stabilized the thermal chamber to these temperatures for several hours for each measurement. We refer to this as the static measurement. In the literature, both methods are used, but they can lead to different results due to the visco-elastic properties of the fiber coating, which causes a delay between the temperature change and the optical phase change [20]. This is highly undesired in the compensated delay-line interferometer, as this delay may be different in the two arms, possibly causing poor compensation of the phase change when the temperature is changing. This delay can be strongly suppressed when fibers with a thin coating are used [20], justifying our choice of thinly-coated HCF and SSMF.

III. Results and Their Analysis

A. Thermal sensitivities of delay-line interferometers

The result of dynamic thermal sensitivity measurement of the compensated delay-line interferometer is shown in Fig. 3. The accumulated phase firstly decreased, reaching a turning point at around 28°C, corresponding to S_φ=0, then increased.

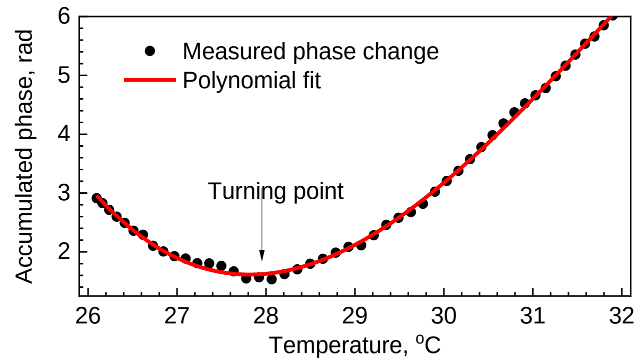

Fig. 3. Dynamically measured phase change of the compensated delay-line interferometer from 26°C to 32°C (black scatter points), and the 3rd order polynomial fit (red line).

To compare delay-line interferometers made of SSMF, HCF and our compensated delay-line interferometer, we normalize the interferometer thermal phase sensitivity to unit delay:

$$I_\varphi = \frac{1}{\tau}\frac{d\varphi}{dT}, \tag{2}$$

where τ is the delay introduced by the delay-line interferometer and φ is the phase difference of the two arms. The delay-normalized thermal sensitivities I_φ of our compensated delay-line interferometer together with those of T-SSMF and T-HCF measured with the dynamic method are plotted in Fig. 4. Here we see that I_φ of T-HCF (~0.5 rad/ns/K) is about 16 times smaller than that of T-SSMF (~8 rad/ns/K). It is worth mentioning that the T-SSMF sensitivity is slightly smaller than that of SSMF reported to have S_φ = 48 rad/m/K, which is a value corresponding to I_φ = 9.6 rad/ns/K. For the compensated delay-line interferometer, I_φ measured over the temperature range of 25-55 °C is almost 7 times smaller than that of T-HCF and over 100 times lower than that of T-SSMF. Additionally, it crosses zero (detail shown in Fig. 5) at 28°C, where the interferometer is essentially thermally insensitive.

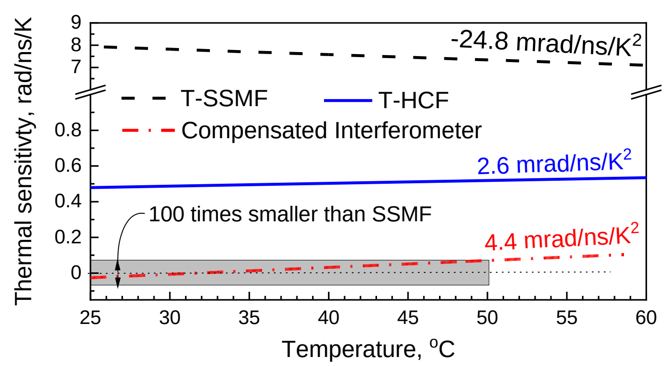

Fig. 4. Measured thermal sensitivity of T-SSMF (black, dashed), T-HCF (blue, solid), and the compensated delay-line (dash-dot, red) interferometers, measured from 25 to 60°C. The shown numbers refer to the slopes of the corresponding curves.

To verify the obtained results, we carried out the static measurement for the compensated interferometer over four temperature ranges (25-27°C, 27-29°C, 29-31°C, and 31-33°C), Fig. 5. Both dynamic and static measurements agree well and show that the thermal phase sensitivity of the compensated delay-line interferometer crossed zero at 28°C. In the temperature range of 27-29°C in which the interferometer can be kept using, e.g., a simple closed-loop temperature control of ±1 K, the interferometer achieves $|I_{\varphi}| < 4.8$ mrad/ns/K, which is over 2000 times lower than that of SSMF-based interferometer.

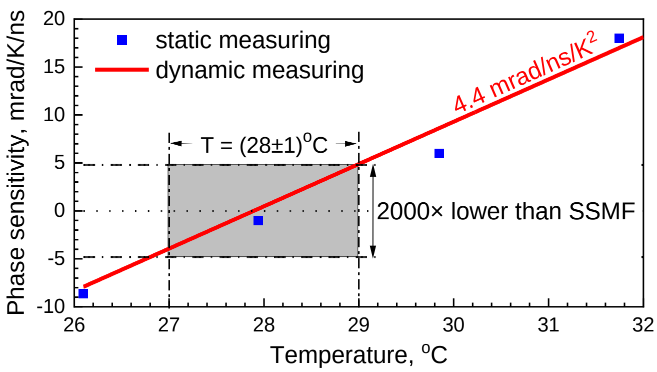

Fig. 5. The dynamically measured (red line) and statically measured (black scatter points) thermal phase sensitivity of the compensated delay-line interferometer. Both show the zero thermal phase sensitivity crossing at a temperature of 28°C.

B. Tuning of the zero thermal sensitivity crossing temperature

Zero thermal interferometer sensitivity was achieved at a particular temperature (28°C in our experiment) as both, T-HCF and T-SSMF exhibit a temperature dependent S_{φ}, which can be seen in Fig. 4. This zero sensitivity temperature can be shifted by changing the length of the fibers. It is more practical to change the T-SSMF fiber length, as it has a large thermal sensitivity coefficient and thus only small changes in its length produce an appreciable shift in the interferometer zero thermal phase sensitivity temperature without changing significantly the delay produced in the compensated delay-line interferometer. 6. shows experimental data obtained when changing the T-SSMF length. We see that a change in the T-SSMF length of 20 cm shifted the zero sensitivity point from 27 to 47°C. Thus, setting the zero sensitivity with ±1°C accuracy requires control of the T-SSMF length of ±1 cm, which is easy-to-achieve with a standard fiber cleaver and splicer. Further modification of the length imbalance beyond what we show here should enable us to lower the zero sensitivity point down to -71°C (for zero length T-SSMF) [13] or to increase it beyond 47°C.

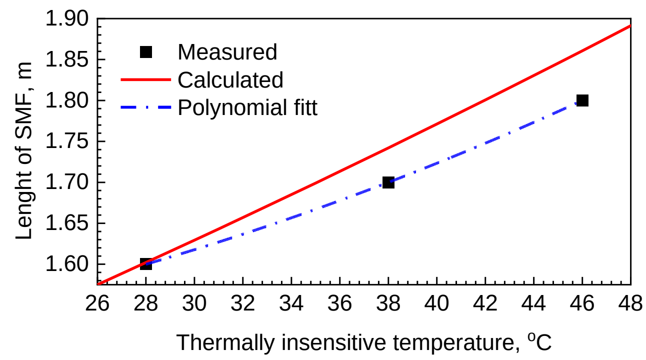

Fig. 6. The measured (black scatter), fitted (2nd order polynomial fit, blue dash-dot) and calculated (red solid, Eq.(4)) relationship between the T-SSMF length and compensated delay-line interferometer zero thermal sensitivity temperature when the T-HCF branch is kept 40 m.

In practice, it is desirable to achieve a very low interferometer thermal sensitivity over as large a temperature range as possible. This requires the interferometer thermal phase sensitivity slope (Fig. 5) to be as small as possible. This slope can be calculated using simple algebra from thermal sensitivity coefficient slopes a of T-HCF and T-SSMF defined as:

$$S_{\varphi}(T) = a(T - T_{room}) + S_{\varphi_{room}}, \tag{3}$$

where T_{room} is room temperature, and S_{φ_room} is the thermal sensitivity coefficient at room temperature. Data shown in Fig. 4 lead to a_{T-SSMF} = -0.12 rad/m/K² (corresponding to -24.8 mrad/ns/K²) and a_{HCF} = 8.5 mrad/m/K² (2.6 mrad/ns/K²), respectively, from which we calculated the slope of the compensated interferometer thermal sensitivity of 4.4 mrad/ns/K². This value agrees with the slope obtained by linear fitting of the compensated delay-line interferometer thermal sensitivity shown in Fig. 4.

The obtained thermal sensitivity coefficient slopes of T-SSMF and T-HCF also allow us to calculate the extra length of T-SSMF that should be added to increase the zero thermal phase sensitivity temperature of the compensated delay-line interferometer by $\Delta T = T - T_{room}$:

$$\Delta L_{SSMF} = \frac{a_{HCF}\Delta T + S_{\varphi\_room_{HCF}}}{a_{T-SSMF}\Delta T + S_{\varphi\_room_{T-SSMF}}} \times L_{HCF}. \tag{4}$$

We plot this dependence in Fig. 6 (red solid). Compared to the measured data (6. , black scatter points), it gives a slightly larger slope, which we believe is due to the too large temperature range considered (from 28 to 46°C), over which the thermal sensitivity coefficients of T-SMF and T-HCF are no longer linear.

To obtain a smaller thermal sensitivity slope (than that obtained in Fig. 4) and thus lower thermal sensitivity over a larger temperature range, a_{T-SSMF} and a_{HCF} would need to be better "matched", e.g., to have the same sign. We believe this can be achieved, e.g., by a careful selection of the dopants in the T-SSMF fiber core or a different choice of coating material (e.g. metallic or polyimide).

C. Wavelength dependence

All our experiments were performed with laser source emitting at 1558 nm. Here, we predict how the compensated delay-line interferometer thermal sensitivity changes with the operation wavelength. The wavelength-dependent thermal sensitivity coefficient of an optical fiber can be written as:

$$S_{\varphi}(\lambda) = \frac{2\pi}{\lambda}\left(\frac{dn_{eff}}{dT}(\lambda) + \frac{n_{eff}(\lambda)}{L}\frac{dL}{dT}\right). \quad (5)$$

The first term of the right hand side is the wavelength dependent thermo-optic effect and the second term is related to the fiber chromatic dispersion and thermally-induced expansion. The thermo-optic effect in a sealed HCF is very weak [14] and for SSMF, it can be described by expansion [22]:

$$\frac{dn}{dT}(\lambda) = c_0 + c_1\lambda^{-2} + c_2\lambda^{-4} + c_3\lambda^{-6}, \quad (6)$$

with $c_{0,1,2,3} = 9.39059;\ 0.235290;\ -1.31856 \times 10^{-3};\ and\ 3.02887 \times 10^{-4}$. The calculated $S_{\varphi}(\lambda)$ (Eq.(5)) of SSMF and HCF considering this dependence, $n_{eff}(\lambda)$ of both fibers calculated in COMSOL Multiphysics, and $\frac{dL}{dT} = 0.3$ ppm/K [20], is shown in Fig. 7. Using these data, the wavelength dependent thermal sensitivity of the compensated delay-line interferometer is calculated and shown in Fig. 8.

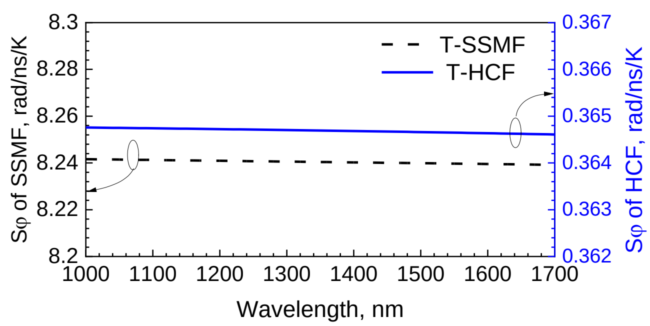

Fig. 7. Calculated wavelength-dependent thermal sensitivity coefficient of T-SSMF and T-HCF.

The thermal sensitivity is within ± 4.8 μrad/ns/K between 1420 and 1660 nm (240 nm span), which is over 2×10^6 times smaller than that of the SSMF based interferometer. Unfortunately, we could not confirm this experimentally, as we did not have a tunable laser that could be locked to the optical frequency comb.

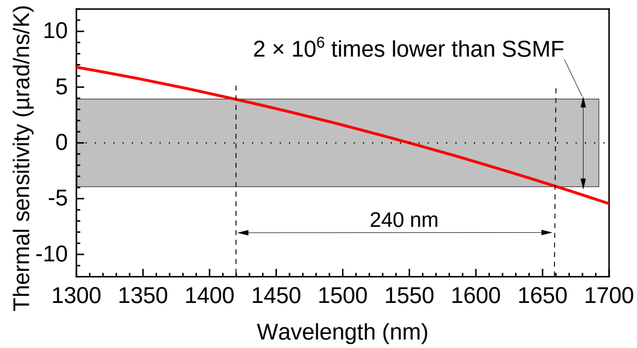

Fig. 8. Calculated thermal sensitivity of the compensated delay-line interferometer as a function of wavelength with zero thermal sensitivity set to 1550 nm.

IV. Conclusion

In conclusion, we have proposed and demonstrated a fiber delay-line interferometer made from HCF and SSMF, with an extremely low thermal sensitivity that crosses zero at a designed temperature. This zero temperature crossing was tuned from 28°C to 45°C via control of the SSMF length in our demonstration. Compared with an SSMF based interferometer, the compensated delay-line interferometer shows about 100 times lower thermal sensitivity in a large temperature range (e.g., 25-50°C). Over a limited temperature range of 2°C, it achieves thermal sensitivity over 2000 times lower than its SSMF based counterpart and 100 times lower than HCF-only interferometer embodiment. Such temperature stability of ±1°C is straightforwardly achievable using a low-cost temperature control system or in a temperature-controlled lab environment. We also discussed the thermal slope of the compensated interferometer and fibers, which approximately gives the relationship between the thermally insensitive temperature and the length of the SSMF. We have also predicted how the thermal sensitivity changes with wavelength, showing the compensated interferometer is expected to achieve 2×10^6 lower sensitivity than its SSMF counterpart even when the wavelength is tuned by as much as 240 nm. Our future work will focus on further reduction of the interferometer thermal sensitivity slope to extend the greatly reduced sensitivity over a larger temperature range. The presented compensated delay-line interferometer will be of interest in applications like stable laser locking or measurement of laser phase drifts due to temperature.

Acknowledgment

This data is accessible through the University of Southampton research repository (DOI: 10.5258/SOTON/D****) [23].

References

[1] Y. T. Chen, "Use of single-mode optical fiber in the stabilization of laser frequency," *Applied optics*, vol. 28, no. 11, pp. 2017-2021, 1989.

[2] H. Stoehr, F. Mensing, J. Helmcke, and U. Sterr, "Diode laser with 1 Hz linewidth," Optics letters, vol. 31, no. 6, pp. 736-738, 2006.
[3] A. P. Luo, Z.-C. Luo, and W.-C. Xu, "Tunable and switchable multiwavelength erbium-doped fiber ring laser based on a modified dual-pass Mach-Zehnder interferometer," *Optics letters*, vol. 34, no. 14, pp. 2135-2137, 2009.
[4] D. Shaddock, "Space-based gravitational wave detection with LISA," *Classical and Quantum Gravity*, vol. 25, no. 11, p. 114012, 2008.
[5] C. Eisele, A. Y. Nevsky, and S. Schiller, "Laboratory test of the isotropy of light propagation at the 10^{-17} level," *Physical Review Letters*, vol. 103, no. 9, p. 090401, 2009.
[6] N. Lagakos, J. Bucaro, and J. Jarzynski, "Temperature-induced optical phase shifts in fibers," *Applied optics*, vol. 20, no. 13, pp. 2305-2308, 1981.
[7] E. Numkam Fokoua, M.N. Petrovich, T.D. Bradley, F. Poletti, D.J. Richardson, and R. Slavík, "How to make the propagation time through an optical fiber fully insensitive to temperature variations," *Optica*, vol. 4, no. 6, pp. 659-668, 2017.
[8] R. Slavík *et al.*, "Ultralow thermal sensitivity of phase and propagation delay in hollow core optical fibres," *Scientific reports*, vol. 5, p. 15447, 2015.
[9] M. Bousonville *et al.*, "New phase stable optical fiber," in *Proc. Beam Instrum. Workshop*, 2012, pp. 101-103.
[10] P. Dragic, M. Cavillon, and J. Ballato, "On the thermo-optic coefficient of P_2O_5 in SiO_2," *Optical Materials Express*, vol. 7, no. 10, pp. 3654-3661, 2017.
[11] Z. Feng *et al.*, "Fiber interferometry with low temperature sensitivity," in *2020 IEEE Photonics Conference (IPC)*, 2020: IEEE, pp. 1-2.
[12] W. Zhu *et al.*, "The thermal phase sensitivity of both coated and uncoated standard and hollow core fibers down to cryogenic temperatures," *Journal of Lightwave Technology*, vol. 38, no. 8, pp. 2477-2484, 2019.
[13] W. Zhu *et al.*, "Temperature insensitive fiber interferometry," *Optics Letters*, vol. 44, no. 11, pp. 2768-2770, 2019.
[14] R. Slavík *et al.*, "Demonstration of opposing thermal sensitivities in hollow-core fibers with open and sealed ends," *Optics letters*, vol. 44, no. 17, pp. 4367-4370, 2019.
[15] M. Ding, E. R. N. Fokoua, T. D. Bradley, F. Poletti, D. J. Richardson, and R. Slavík, "Hollow core fiber temperature sensitivity reduction via winding on a thermally-insensitive coil," in *CLEO: Science and Innovations*, 2021: Optical Society of America, p. STu1Q. 7.
[16] L. Tang, Y. Li, J. Li, S. Yang, H. Chen, and M. Chen, "Temperature-insensitive Mach–Zehnder interferometer based on a silicon nitride waveguide platform," *Optics letters*, vol. 45, no. 10, pp. 2780-2783, 2020.
[17] B. Shi *et al.*, "Temperature-insensitive delay-line fiber interferometer," in *CLEO: Science and Innovations*, 2021: Optical Society of America, p. STu2A. 4.
[18] F. Poletti, "Nested antiresonant nodeless hollow core fiber," *Optics express*, vol. 22, no. 20, pp. 23807-23828, 2014.
[19] S. T. Shiue and Y.-K. Tu, "Relaxation of thermal stresses in double-coated optical fibers," *Journal of applied physics*, vol. 86, no. 8, pp. 4085-4090, 1999.
[20] B. Shi *et al.*, "Thinly coated hollow core fiber for improved thermal phase-stability performance," *Optics Letters*, vol. 46, no. 20, pp. 5177-5180, 2021.
[21] K. Koo, A. Tveten, and A. Dandridge, "Passive stabilization scheme for fiber interferometers using (3× 3) fiber directional couplers," *Applied Physics Letters*, vol. 41, no. 7, pp. 616-618, 1982.
[22] R. E. Bartolo, A. B. Tveten, and A. Dandridge, "Thermal phase noise measurements in optical fiber interferometers," IEEE Journal of Quantum Electronics, vol. 48, no. 5, pp. 720-727, 2012.
[23] B. Shi, G. Marra, Z. Feng, H. Sakr, J.R. Hays, E. Numkam Fokoua, M. Ding, F. Poletti, D.J. Richardson, and R. Slavík, Dataset, University of Southampton Institutional Repository (2021), https://doi.org/10.5258/SOTON/xxxx